PHYSICAL REVIEW B VOLUME 15, NUMBER 4 15 FEBRUARY 1977

Plasmon and polar optical phonons in reduced rutile TiO_{2-x}

Jean-François Baumard and François Gervais
Centre de Recherches sur la Physique des Hautes Températures, Centre National de la Recherche Scientifique, 45045 Orléans, France
(Received 1 October 1976)

The infrared reflectivity of reduced rutile TiO_{2-x} at room temperature is reported at departures x from stoichiometry varying from 10^{-3} to 5×10^{-2}. The electron carriers resulting from the lattice defects are responsible for a plasmon mode which couples with the longitudinal-optical phonon modes. A suitable model for the dielectric function involving a factorized form for the pure-phonon modes added to a plasmon contribution allows a good fit of calculated spectra to experimental data and is of special interest to decouple observed excitations into elementary phonon and plasmon modes. The parameters entering the decoupled phonon modes are then discussed in relation to the case of stoichiometric rutile, while a simple linear relation is found between the plasma frequency squared and the sample composition at room temperature. The plasma frequency rises for a small increase of temperature and it is concluded that activation of carriers to the conduction band should constitute the essential feature of the electrical-conductivity transport mechanism.

I. INTRODUCTION

Several investigations concerning the transport properties of TiO_2 rutile connected with the defect structure at high temperature revealed that the chemical equilibrium between the solid and a reducing gas phase leads to a significant loss of oxygen.[1] While the situation at high temperature is not entirely clear,[1] careful structural observations have shown that the departure from stoichiometry in rutile in the vicinity of room temperature is mainly accommodated by extended defects, via a crystallographic shear mechanism. This has been the subject of extensive reviews[2] and will not be further developed here. Such an ability to lose oxygen has been frequently used in the past to investigate transport properties, simply because the resulting lattice defects affect the number of available carriers and consequently govern related properties, especially electrical conductivity. However, an unequivocal distinction between the respective contributions of electronic concentration and carrier mobility cannot be made from the simple temperature dependence of the electrical conductivity alone. As the variation of the electron mobility with temperature is an important feature of the transport mechanism, some conflict stemming from a different estimate of the two contributions has been raised in the literature.[3]

As a straightforward consequence of the oxygen loss, while nominally stoichiometric rutile has insulating properties at low or moderate temperature, the absorption coefficient in the transparent regime was shown recently to increase with temperature[4] above 1000 K in such a way that the laws of multiphonon absorption[5] fail to describe the observed temperature dependence. A plausible explanation lies in free-carrier absorption resulting from the lattice disorder. This would not be the case in Al_2O_3 corundum, for instance, where chemical stability insures a constant composition in usual experimental conditions and where absorption by electronic charge carriers plays a minor role in the 1000–2500-cm^{-1} frequency range. The temperature dependence of the infrared-active vibrational modes in stoichiometric rutile has been published recently with emphasis on ferroelectric properties.[6] As long as the concentration of the free carriers is not too low in this material, a coupling between a plasmon mode and the longitudinal-optical (LO) phonon modes is expected to be observed. In the present paper the infrared reflection spectra of reduced rutile TiO_{2-x} with departures from stoichiometry greater than 10^{-3} are reported. A new dielectric-function model derived from the factorized form is introduced and allows a decoupling of the observed LO excitations into pure LO phonon and pure plasmon. Thus the frequencies and dampings of the uncoupled TO and decoupled LO phonon modes may be compared to those found in stoichiometric rutile,[6] while conclusions can be drawn about the physical parameters which fix the plasma frequency for a given sample composition.

II. EXPERIMENTAL

Rutile single crystals were cut from a boule grown by the Verneuil technique and supplied by Hrand Djevahirdjian S. A. Samples used were monocrystalline disks, the geometrical axes of which are parallel to the $\vec{c}$ axis. The crystals were polished and then treated under appropriate reducing conditions at temperatures between 1500 and 1600 K,[1] to ensure variable compositions, then quenched to room temperature in an argon atmo-

sphere to avoid surface reoxidation. The crystals were then optically polished with alumina powder. The composition of the sample was determined by reoxidation in oxygen in a microbalance. Special care was devoted to the temperature and annealing times to get homogeneous samples in order that the bulk composition given by the above stoichiometry analysis should be maintained over the infrared penetration depth. Optical polishing after the reducing treatment removes any reoxidation of the surface during quenching, owing to the fact that reduced TiO_{2-x} reacts rapidly with oxygen even at moderate temperatures. Despite this care, some dispersion of the results when they are plotted versus composition may be due to experimental difficulties. The infrared reflection spectra were recorded in the conditions previously reported by Gervais *et al.*[6]

III. INFRARED REFLECTIVITY DATA AND ANALYSIS

The infrared reflectivity of several TiO_{2-x} samples for the ordinary ray ($\vec{E} \perp \vec{c}$) is shown in Figs. 1 and 2 and compared with the reflection spectrum of stoichiometric TiO_2 in Fig. 1. A Kramers-Kronig analysis cannot be performed for lack of data at frequencies below 280 cm^{-1}.

The failure of the classical dispersion theory

$$\epsilon = \epsilon_\infty + \sum_j \Delta\epsilon_j \Omega_{jTO}^2 / (\Omega_{jTO}^2 - \omega^2 + i\gamma_{jTO}\omega) \qquad (1)$$

applied to the reflection of rutile has been emphasized previously.[6,7] The reasons will be outlined below. For a single reflection band ($j=1$), the structure of the transverse optical mode is given by the imaginary part of the dielectric function,

$$\mathrm{Im}(\epsilon) = \Delta\epsilon\,\Omega_{TO}^2\gamma_{TO}\omega / [(\Omega_{TO}^2 - \omega^2)^2 + \gamma_{TO}^2\omega^2] \ , \qquad (2)$$

and the structure of the longitudinal one by the imaginary part of the inverse dielectric function,

$$\mathrm{Im}\left(\frac{1}{\epsilon}\right) = \frac{\Delta\epsilon}{\epsilon_\infty^2} \frac{\Omega_{TO}^2\gamma_{TO}\omega}{(\Omega_{LO}^2 - \omega^2)^2 + \gamma_{TO}^2\omega^2} \ . \qquad (3)$$

Formulas (2) and (3) still hold for an isolated band or for the strongest band of a spectrum if all other bands are much weaker. It is seen from a comparison of Eqs. (2) and (3) that the width at half-height of the LO peak, that is, the LO damping, is nothing else than γ_{TO}. Consequently, whereas the classical dispersion theory may be adequate to describe a *narrow* reflection band when both TO- and LO-mode energies are neighboring and thus approximately the same phonon decays are expected, there is no reason for an identity between γ_{TO} and γ_{LO} when the LO-mode energy is well above the TO one, that is when the reflection band is wide.[7] This is the case in rutile since $\Omega_{TO} = 189$ cm^{-1}, while $\Omega_{LO} = 831$ cm^{-1} for the strongest polar mode of the E_u type.[6]

A treatment of the anharmonic lattice dynamics with the aid of phonon Green's functions[8] yields the quantum analog of Eq. (1) in terms of a sum of phonon propagators of the form

$$G(\vec{0}j, \omega) \sim \frac{1}{\omega^2(\vec{0}j) + 2\omega(\vec{0}j)\Delta\omega(\vec{0}j, \omega) - \omega^2 + 2\omega(\vec{0}j)\Gamma(\vec{0}j, \omega)} \qquad (4)$$

weighted by dipolar moment factors. The optical-phonon mode is defined by its branch index j and wave vector $\vec{k} \simeq \vec{0}$ in standard notation.[8] In Eq. (4), both frequency shift $\Delta\omega$ and damping 2Γ are frequency-dependent functions. The evaluation of the damping function in the vicinity of the LO frequency

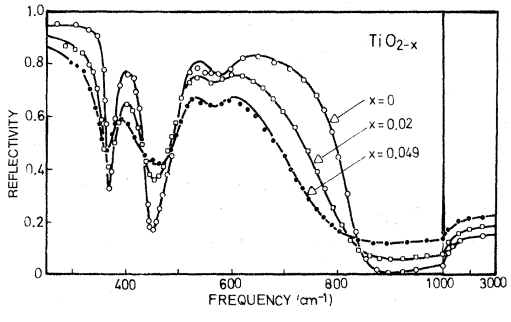

FIG. 1. Infrared reflectivity spectrum for the ordinary ray of stoichiometric rutile (open circles) compared with that of nonstoichiometric compounds (other symbols). The best fit (full curves) to the data with the aid of the dielectric function model Eq. (11).

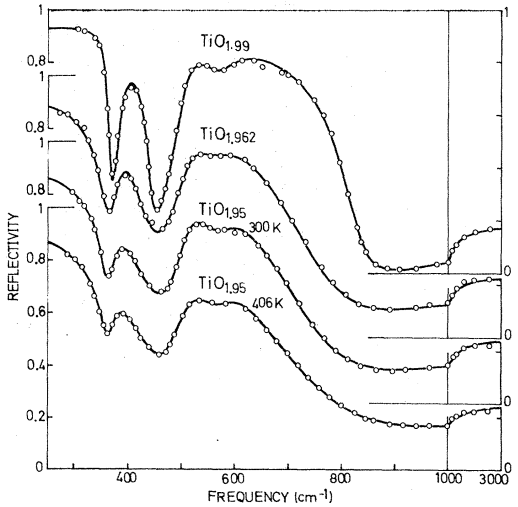

FIG. 2. The dependence of the infrared reflectivity of rutile TiO_{2-x} (ordinary ray) on the departure from stoichiometry. Circles are experimental points. Full curves are the best fit of Eq. (11) to the data.

determines the width at half-height of the LO peak. However, Eq. (4) would be usable only if one could calculate *ab initio* the phonon self-energy terms $\Delta\omega(\vec{0}j,\omega)$ and $\Gamma(\vec{0}j,\omega)$. Such an eventuality is questionable in rutile at the present time.

The factorized form of the dielectric function[9]

$$\epsilon=\epsilon_\infty\prod_j\left[(\Omega_{j\mathrm{LO}}^2-\omega^2+i\gamma_{j\mathrm{LO}}\omega)/(\Omega_{j\mathrm{TO}}^2-\omega^2+i\gamma_{j\mathrm{TO}}\omega)\right], \tag{5}$$

also called the four-parameter model,[7] is appropriate to describe the reflection spectrum of rutile.[6,7] This model involves constant, but possibly unequal, dampings for the TO and LO modes, and makes an assumption about the form of the damping function. When $j=1$ and neglecting terms of order γ^2, a combination of Eqs. (4) and (5) yields

$$2\omega(\vec{0}j)\Gamma(\vec{0}j,\omega)=\omega\{\gamma_{\mathrm{TO}}-(\gamma_{\mathrm{LO}}-\gamma_{\mathrm{TO}})[(\Omega_{\mathrm{TO}}^2-\omega^2)/(\Omega_{\mathrm{LO}}^2-\Omega_{\mathrm{TO}}^2)]\}, \tag{6}$$

that is, a monotonic increase of the damping function from a value γ_{TO} at $\omega=\Omega_{\mathrm{TO}}$ up to another value γ_{LO} at $\omega=\Omega_{\mathrm{LO}}$.[7]

A system of plasmon-phonon coupled modes can be treated as an optical phonon system with one excitation, the transverse frequency of which should be zero. Equation (5) with one of the $\Omega_{j\mathrm{TO}}$ frequencies set equal to zero combined with

$$R=|(\epsilon^{1/2}-1)/(\epsilon^{1/2}+1)|^2 \tag{7}$$

fits the present reflectivity data satisfactorily. This procedure has been used recently in other semiconductor compounds.[10]

But the phenomenon of LO-phonon–plasmon coupling, although interesting in itself, masks the individual properties of the plasmon and the phonons in TiO_{2-x}. A method of decoupling the system is to decompose the dielectric function into a sum of two terms: (i) a pure-phonon contribution given by Eq. (5) which has the advantage of describing the phonon reflectivity correctly, and (ii) a pure-plasmon contribution. The discussion above which concerns phonons and their description in accordance with infrared reflectivity data, holds for a plasmon mode as well. Equation (5) applied to a plasmon mode is written in the form

$$\epsilon_{\mathrm{pl}}=\epsilon_\infty\frac{\Omega_p^2-\omega^2+i\gamma_p\omega}{-\omega^2+i\gamma_0\omega}, \tag{8}$$

$$\epsilon_{\mathrm{pl}}=\epsilon_\infty\left(1-\frac{\Omega_p^2+i(\gamma_p-\gamma_0)\omega}{\omega(\omega-i\gamma_0)}\right). \tag{9}$$

Equation (8) makes a distinction between the damping γ_p at the plasma frequency and the "static" damping γ_0. This is an improvement with respect to the Drude formula, which is nothing else than Eq. (9) with the restriction $\gamma_p=\gamma_0$. The application of Eq. (6) to the plasmon case indicates that the present model assumes the form

$$\gamma_{\mathrm{pl}}(\omega)=\gamma_0+(\gamma_p-\gamma_0)\omega^2/\Omega_p^2 \tag{10}$$

for the plasmon damping function. A quantity ϵ_∞ which is already incorporated into the lattice term should be deduced from Eq. (9) to obtain the plasmon contribution. Equation (5) is thus rewritten in the equivalent form

$$\epsilon=\epsilon_\infty\left(\prod_{j,\mathrm{ph}}\frac{\Omega_{j\mathrm{LO}}'^2-\omega^2+i\gamma_{j\mathrm{LO}}'\omega}{\Omega_{j\mathrm{TO}}^2-\omega^2+i\gamma_{j\mathrm{TO}}\omega}-\frac{\Omega_p^2+i(\gamma_p-\gamma_0)\omega}{\omega(\omega-i\gamma_0)}\right), \tag{11}$$

where the primes indicate pure-lattice LO modes. Best fits of Eq. (11) to experimental data are shown in Figs. 1 and 2. Parameters used are given in Table I for $TiO_{1.95}$ as an example and compared with results found in TiO_2. Results are plotted in Figs. 3–7 for other samples. TO phonon

TABLE I. Uncoupled-mode parameters used to fit infrared reflectivity data of $TiO_{1.95}$ with Eq. (11). Oscillator strengths are indicated but are not used in the fit. A secondary oscillator[6] taken into account in the fit is omitted in the table for clarity. Coupled-mode parameters are deduced from the dielectric function Eq. (11) when the fit is achieved. All frequencies and dampings are expressed in cm^{-1} unit.

TiO_2			$TiO_{1.95}$	
Transverse modes				
$\Delta\epsilon_j$	$\Omega_{j\mathrm{TO}}$	$\gamma_{j\mathrm{TO}}$	$\Omega_{j\mathrm{TO}}$	$\gamma_{j\mathrm{TO}}$
70.2	189	27	(189)	53
0.9	381.5	16.5	374	30
2.6	508	24	511	43
Longitudinal modes				
		Pure lattice		Coupled modes
$\Omega_{j\mathrm{LO}}$	$\gamma_{j\mathrm{LO}}$	$\Omega'_{j\mathrm{LO}}$	$\gamma'_{j\mathrm{LO}}$	$\Omega_{j\mathrm{LO}}$	$\gamma_{j\mathrm{LO}}$
367	10	355	15	357.5	31
443.5	21.5	427	70	440	80
831	50	709	70	790	255
High-frequency dielectric constant					
6.0			9.3		
			Plasmon parameters		
		γ_0	Ω_p		γ_p
		825	530		850
			Additional mode		
		Ω_{TO}	Ω_{LO}		γ
		482	480		(40)

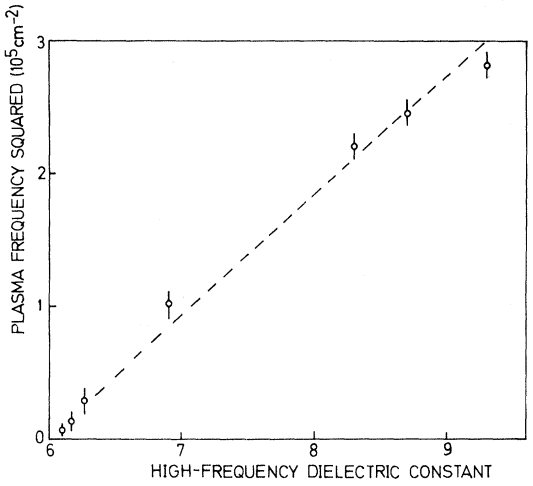

FIG. 3. A plot of the square of the plasma frequency vs the high-frequency dielectric constant. Both quantities have the dimension of an oscillator strength or behave like and the curve is consistently found to be nearly straight.

modes are the complex poles of Eqs. (5) and (11) and identical TO parameters are found. The best fit with Eq. (5) would provide the parameters of LO phonon-plasmon coupled modes. But such coupled-mode frequencies and dampings also are the moduli and twice the imaginary parts of the complex zeros of Eq. (11), respectively. Both procedures are strictly equivalent. Coupled-mode

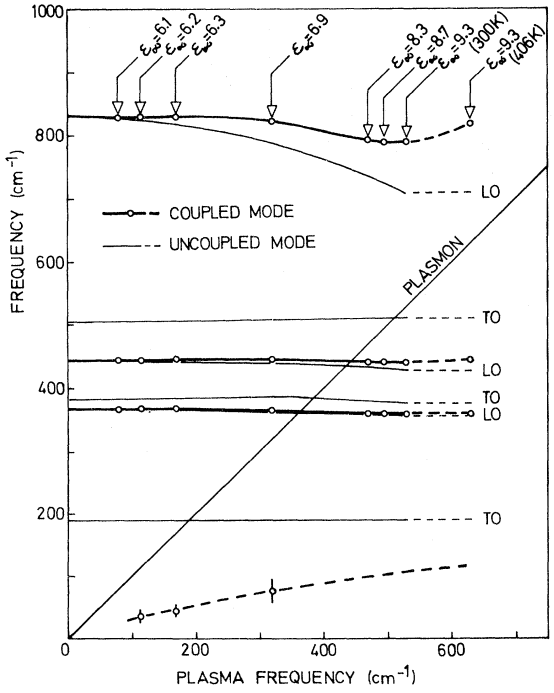

FIG. 5. Plasmon-phonon dispersion curve.

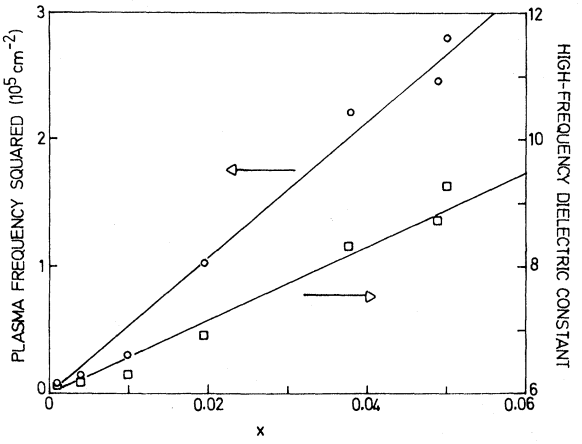

FIG. 4. The dependences of the square of the plasma frequency and the high-frequency dielectric constant on the departure x from stoichiometry.

parameters are thus given in Table I and Figs. 5–7.

IV. DISCUSSION OF THE RESULTS

A. TO and decoupled LO phonon modes

An increase of ϵ_∞ with x is found. This is readily observed as a rise of the reflectivity level at high frequency (Figs. 1 and 2). This increase shifts pure-lattice LO frequencies towards low frequencies according to

$$\Omega_{LO}^2 = \Omega_{TO}^2(1 + \Delta\epsilon/\epsilon_\infty) \tag{12}$$

for a single mode. TO frequencies are found independent of x within 2% for the 381-cm^{-1} mode

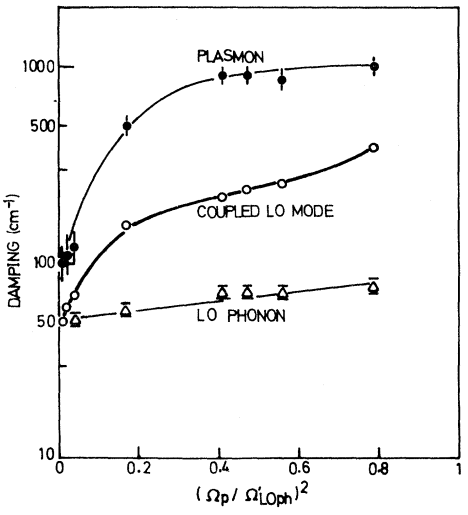

FIG. 6. A comparison of dampings of the highest-frequency LO phonon, the plasmon, and the LO-phonon–plasmon coupled mode.

and within 1% for the more intense mode at 508 cm^{-1} (Fig. 5). Owing to the weak TO-LO splitting of the 381-cm^{-1} mode, the parameters of this mode are rather inaccurate, however. Oscillator strengths of the three polar modes as given in Table I and determined from TO-LO splittings in stoichiometric rutile,[6] are assumed to be also independent of x so that Ω'_{jLO} frequencies can be calculated on these bases. One verifies that the pure-lattice LO frequencies calculated from the generalization of formula (12) including damping and from the oscillator strengths given in Table I agree with those entered as fit parameters in obtaining the results shown in Figs. 1 and 2 within 2% for the 367-cm^{-1} mode and within 1% for the 443-cm^{-1} mode. Such a result gives support to the assumption of oscillator strengths nearly independent of x. An additional phonon mode seems to appear for a departure from stoichiometry higher than 4%. Its frequency would be 480 ± 5 cm^{-1} and its oscillator strength is weak (~0.1).

An increase of pure-phonon dampings with x is observed. This rise is monotonic and reaches 10–50 cm^{-1} depending on the mode. An example of this effect is seen in Figs. 6 and 7. One may wonder whether disorder introduced by nonstoichiometry is responsible alone for this additional contribution to the mode damping. It is possible, for instance, that anharmonic couplings with electronic excitations also play a part. Figure 2 shows the infrared reflectivity of the most reduced sample on heating at 406 K. Measurements at higher temperature have not been performed to avoid re-

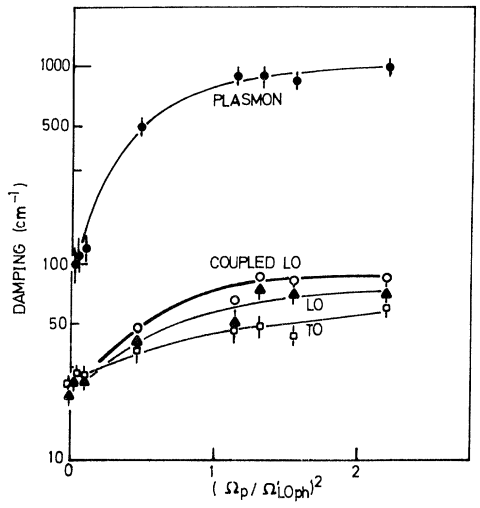

FIG. 7. A comparison of dampings of the 508-cm^{-1} TO phonon, the 443-cm^{-1} LO phonon, the plasmon, and the LO-phonon–plasmon coupled mode. Results show that the coupled mode remains essentially phononlike even beyond the plasmon-phonon frequency crossing.

oxidation. The sample composition is verified to be unchanged at 406 K since ϵ_∞ remains a constant. Phonon dampings are only slightly affected by heating. A damping increase due to filling of phonon levels nevertheless is expected according to laws determined in the stoichiometric compound.[6] Results indicate that such an increase is counterbalanced by another phenomenon which cannot be other than a partial structural arrangement as a consequence of annealing. Disorder, then, would appear as the major cause of the additional damping in reduced rutile. The fact that this additional damping fluctuates around a medium value depending on the sample preparation for a same composition also supports this idea.

B. Plasmon and carrier effective mass

The structure of the decoupled plasmon mode is shown in Figure 8 for several values of x. It should be pointed out, however, that plasmon parameters are determined with little accuracy when the plasma frequency is lower than 300 cm^{-1}, that is, outside the spectral range available with our apparatus. The simultaneous rise of the plasma frequency and the high-frequency dielectric constant are shown in Fig. 3. Actually the square of the plasma frequency plays the role of an oscillator strength. One verifies in Fig. 3 that Ω_p^2 increases linearly or nearly so with the additional contribution to the former ϵ_∞ dielectric constant measured in stoichiometric TiO_2. This latter contribution is also an oscillator strength associated with transitions in the visible and near-infrared regions. Reduction indeed darkens the crystal. Both quantities Ω_p^2 and ϵ_∞ are plotted versus the departure x from stoichiometry in Fig. 4. The dependences are found roughly linear as may be expected. The plasmon mode is found overdamped $(\gamma_p/\Omega_p > 1/\sqrt{2})$ for any x. Short lifetimes and then high damping are also observed in semiconductor compounds such as CdS, CdTe, GaAs, or GaP.[10] The electronic transport mechanism in rutile has been the subject of a number of previous papers.[3,11] Relatively well-conducting samples were obtained

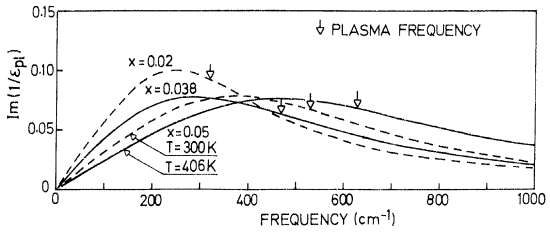

FIG. 8. The imaginary part of the inverse dielectric function (plasma contribution alone) showing the structure of the decoupled plasmon mode.

by reduction of the oxide or doping with suitable agents. However, as the interpretation of Hall effect data in this low-mobility material is rather difficult owing to electron-lattice interactions, much of the experimental evidence rests on the temperature dependence of the electrical conductivity.[3] Unfortunately, the increase of electrical conductivity with temperature may arise from a progressive exhaustion of filled donor levels to the conduction band and/or from an activated drift mobility of carriers. Bogomolov *et al.*[3] in a number of papers assume that the donor levels in reduced rutile are empty beyond ~100 K, and that at higher temperature the variation of electrical conductivity reflects an activated character of electron mobility. From the recent work of Iguchi,[12] one can deduce that the activation energy for conductivity is not dependent upon the degree of reduction and amounts to 0.03 eV or nearly so in the vicinity of room temperature.[12,13] On taking the formulas

$$n = n_0 \exp(-0.03/k_B T), \tag{13}$$

$$\Omega_p^2 = ne^2/m^* \epsilon_\infty , \tag{14}$$

where n denotes the carrier concentration and m^*, the effective electron mass, and where other symbols have their standard meaning, one is able to calculate the variation of the plasma frequency versus temperature in the case of a progressive exhaustion of carriers. This has been checked experimentally for the most heavily reduced sample ($x \sim 0.05$), where a good numerical precision on the plasma frequency is achieved. The experimental variation of Ω_p between 300 and 406 K is 100 cm^{-1}, whereas 90 cm^{-1} is found by means of Eqs. (13) and (14). Such a simple argumentation strongly suggests that the assumption of a complete ionization of donor levels beyond 100 K which supports the idea of a small polaron character of electron carriers in TiO_2, is not valid.[3]

Turning now to the problem of effective mass, an order of magnitude of the carrier concentration may be deduced from the different sample compositions. The dependence of Ω_p^2 on x (Fig. 4) is roughly linear. Then from this relation and Eq. (14), the electronic carrier concentration is simply related to the departure from stoichiometry by a linear law. According to the Seebeck coefficient data of Frederikse,[11] a rough decrease of one order of magnitude for the electronic carrier concentration occurs between exhaustion range and room temperature. Thus on assuming one free electron per $3d^1$ titanium in the exhaustion range at high temperature, one can calculate the values of n at 300 K. They are given in Table II and vary from 6×10^{18} cm^{-3} up to 3×10^{20} cm^{-3}. According to Eq. (14) such data lead to an electron effective mass of (8–10) m_e, which is in good agreement with the value $m^* = 7m_e$ given by Hasiguti.[13]

C. LO-phonon–plasmon coupling

The imaginary part of the dielectric and inverse dielectric functions of a rutile sample where $x = 0.02$ and 0.049 is shown in Fig. 9 and compared with those of the stoichiometric compound. Coupled- and decoupled-mode frequencies are plotted in Fig. 5 versus the plasma frequency. Such a plasmon-phonon dispersion curve has the well-known characteristics of coupling between LO excitations. Other characteristics of mode coupling are seen in Figs. 6 and 7. Coupling indeed manifests itself by a transfer of damping from the uncoupled modes to the coupled mode with an influence which depends on their position with respect to the uncoupled-mode crossing region. This effect is clearly observed for the highest-frequency LO mode, although the crossing region is not yet reached for the maximum plasma frequency in the present investigation. Let us recall that the highest-frequency LO mode in rutile corresponds to the lowest-frequency TO mode. This assignment derives from the inspection of the oscillator strengths of both modes. They are indeed observed to be by far the highest among the three modes for each direction of propagation (Fig. 9). The two minor modes at 381 and 508 cm^{-1}, the TO frequency of which is situated between the TO and LO frequencies of the major mode, have their corresponding LO frequency below their own TO frequency. This is a general phenomenon which is demonstrated in the Appendix. The position of these two minor modes has an important consequence from the point of view of the coupling with the plasmon mode. Each coupled LO mode is shifted from the position of the pure-phonon frequency in a quantity which

TABLE II. Plasmon parameters and quantities that enter the formula $\Omega_p^2 = ne^2/m^*\epsilon_\infty$.

x	0	0.001	0.006	0.01	0.02	0.038	0.049	0.05	0.05
n_{calc}	...	6.4×10^{18}	3.8×10^{19}	6.4×10^{19}	1.3×10^{20}	2.4×10^{20}	3.1×10^{20}	3×10^{20}	4×10^{20}
T				room temperature					406 K
ϵ_∞	6.0	6.1	6.2	6.3	6.9	8.3	8.7	9.3	9.3
Ω_p	0	~80	~115	~170	320	470	495	530	630
γ_p	...	(100)	(110)	(120)	500	900	900	850	1000

does not exceed 19 cm^{-1} for the 443-cm^{-1} mode and only 2.5 cm^{-1} for the 367-cm^{-1} mode. In addition, since the coupling with the plasmon increases the pure-lattice LO mode damping in a quantity which does not exceed 15 and 21 cm^{-1}, respectively, one can say that coupled modes remain essentially phononlike, when this is compared with the situation for the highest-frequency LO mode (Figs. 6 and 7). In other words, the two minor modes appear only weakly coupled to the plasmon mode. This is not surprising because the LO frequencies of these two modes are confined into a "dielectric box." This is due to the proximity of their associated TO frequency towards which they shift asymptotically in order that the sequence transverse-longitudinal-transverse-... should be satisfied in the spectrum, as a result of well-known dielectric considerations.

V. CONCLUSION

The factorized form of the dielectric function appears of a special interest to describe the infrared reflection spectra in reduced rutile TiO_{2-x}, as well as in the stoichiometric compound, owing to the presence of a wide reflectivity band. Moreover, a decoupling of the observed excitations is readily achieved by decomposition of the dielectric function into a sum of independent contributions both derived from the factorized form. Such a model allows a good fit to the reflectivity data and provides the frequencies and dampings of all uncoupled, coupled, and decoupled optical modes. The factorized form of the dielectric function fits the data equally well since this is strictly equivalent for an appropriate choice of parameters, but the decoupling of the system of three polar phonons coupled with a plasmon in the presence of high damping would be difficult to perform mathematically. While TO frequencies are not much affected by the departure from stoichiometry, the coupling between the highest-frequency LO phonon and the plasmon modes leads to significant frequency shift and damping transfer between the two modes. The increase of the pure-phonon damping probably reflects the disorder created by the introduction of lattice defects. The variation of the plasma frequency with temperature clearly supports a progressive ionization of donor levels and suggests some revision of transport property investigations involving an activated electronic drift mobility. Such an approach could be extrapolated to lower and higher temperatures, as long as the plasmon frequency is not too low, and the experimental conditions do not alter the sample composition, respectively.

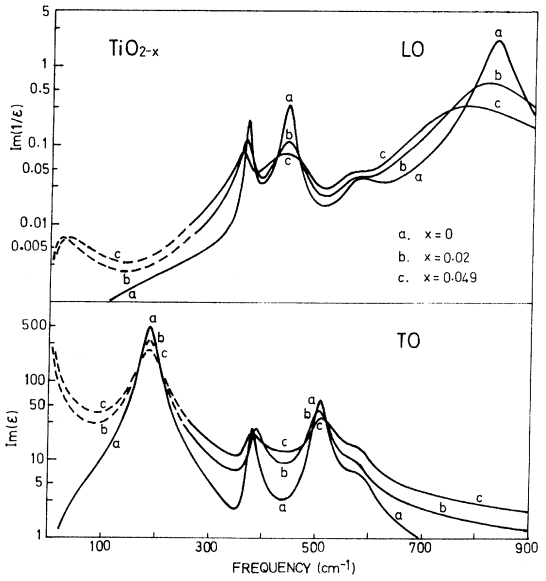

FIG. 9. Imaginary parts of the dielectric and inverse dielectric functions used to fit reflectivity data as shown in Fig. 1, corresponding to the structure of transverse- and longitudinal-phonon–plasmon coupled modes, respectively.

APPENDIX

A polar phonon mode labeled 1, characterized by its TO frequency Ω_{1TO} and its oscillator strength $\Delta\epsilon_1$, is considered. The corresponding LO frequency is given by Eq. (12),

$$\Omega_{1LO} = \Omega_{1TO}(1 + \Delta\epsilon_1/\epsilon_\infty)^{1/2}, \tag{A1}$$

which is a straightforward application of the Lyddane-Sachs-Teller relation. Another weakly polar mode the TO frequency of which, noted Ω_{2TO}, is situated between the TO and LO frequencies of the former mode, is now considered. Resulting LO frequencies are the roots of the equation $\mathrm{Re}(\epsilon) = 0$, that is, from Eq. (1) and neglecting damping

$$\Omega_{LO_\pm} = (1/\sqrt{2})\{\Omega_{1LO}^2 + \Omega_{2LO}^2 \pm [(\Omega_{1LO}^2 + \Omega_{2LO}^2)^2 - 4(\Omega_{1LO}^2\Omega_{2TO}^2 + \Omega_{1TO}^2\Omega_{2LO}^2 - \Omega_{1TO}^2\Omega_{2TO}^2)]^{1/2}\}^{1/2}, \tag{A2}$$

where $\Omega_{2LO} = \Omega_{2TO}(1 + \Delta\epsilon_2/\epsilon_\infty)^{1/2}$.

When $\Delta\epsilon_2 \ll \Delta\epsilon_1$, LO frequencies are given approximately by

$$\Omega_{LO_+}^2 \simeq \Omega_{1LO}^2 + \frac{\Delta\epsilon_1\Delta\epsilon_2}{\epsilon_\infty^2}\,\frac{\Omega_{1TO}^2\Omega_{2TO}^2}{\Omega_{1LO}^2 - \Omega_{2TO}^2}, \tag{A3}$$

$$\Omega_{LO_-}^2 \simeq \Omega_{2TO}^2 - \frac{\Delta\epsilon_2}{2\epsilon_\infty}\,\frac{\Omega_{2TO}^2(\Omega_{1LO}^2 + \Omega_{2TO}^2 - 2\Omega_{1TO}^2)}{\Omega_{1LO}^2 - \Omega_{2TO}^2}. \tag{A4}$$

The second term of the right-hand side of both Eqs. (A3) and (A4) is positive. Consequently, when the oscillator strength of mode 2 begins to grow, the LO_+ frequency of the former mode is shifted towards higher frequencies, while the LO_- frequency of mode 2 is *lower* than its own TO frequency.

ACKNOWLEDGMENTS

Numerical calculations have been performed with the aid of the CII 10070 computer of the C.I.C.R.C. Orléans. Part of this work was performed with the help of G. Prisse. The sample compositions were determined by B. Granier and J. P. Coutures at C.N.R.S., Odeillo.

[1]J. F. Baumard, D. Panis, and A. M. Anthony, J. Solid State Chem. (to be published).

[2]L. A. Bursill and B. G. Hyde, *Progress in Solid State Chemistry* (Pergamon, London, 1972), Vol. 7, p. 177; R. J. D. Tilley, *MTP International Review of Science*, (Butterworth, London, 1975), Ser. 2, Vol. 10, p. 73.

[3]V. N. Bogomolov, E. K. Kudinov, and Yu A. Firsov, Fiz. Tverd. Tela 9, 3175 (1967) [Sov. Phys.-Solid State 9, 2502 (1968)]; V. N. Bogomolov, I. A. Smirnov, and E. V. Shadrichev, Fiz. Tverd. Tela 11, 3214 (1969) . [Sov. Phys.-Solid State 11, 2606, (1970)].

[4]D. Billard, J. Simonato, B. Piriou, High Temp. High Pressures (to be published).

[5]D. Billard, F. Gervais, and B. Piriou, Phys. Status Solidi B 75, 117 (1976); F. Gervais, D. Billard, and B. Piriou, Rev. Hautes Temp. Refract. 12, 58 (1975).

[6]F. Gervais and B. Piriou, Phys. Rev. B 10, 1642 (1974).

[7]F. Gervais and B. Piriou, J. Phys. C 7, 2374 (1974).

[8]A. A. Maradudin and F. E. Fein, Phys. Rev. 128, 2589 (1962); R. A. Cowley, Adv. Phys. 12, 421 (1963).

[9]D. W. Berreman and F. C. Unterwald, Phys. Rev. 174, 791 (1968).

[10]A. A. Kukharskii, Solid State Commun. 13, 1761 (1973); S. Perkowitz and R. M. Thorland, Solid State Commun. 16, 1093 (1975); M. Giehler and E. Jahne, Phys. Status Solidi B 73, 503 (1976).

[11]H. P. R. Frederikse, J. App. Phys. Suppl. 32, 2211 (1961).

[12]E. Iguchi, K. Yagima, T. Asahina, and T. Kanamori, J. Phys. Chem. Solids 35, 597 (1974).

[13]R. R. Hasiguti, E. Yagi, and M. Aono, Radiat. Eff. 4, 137 (1970).